Supporting Information

Defect healing via a gradient cooling strategy for efficient all-inorganic perovskite solar cells

Jiani Lv, Wenning Zhao, Wenhui Li, Jiatao Yu, Mingzhe Zhang, Xiuxun Han* and Tooru Tanaka*

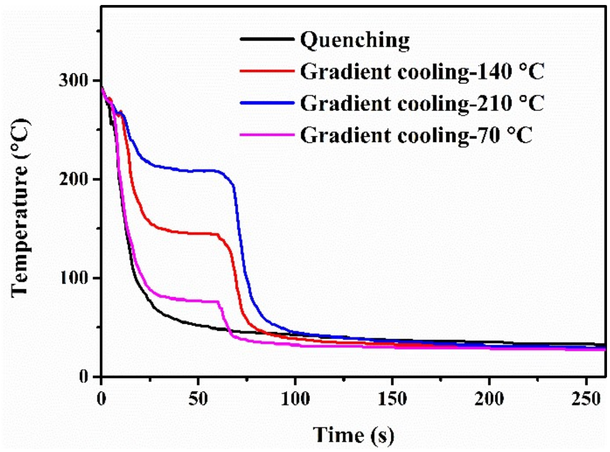

Figure S1. Cooling curves of quenching and gradient cooling processes.

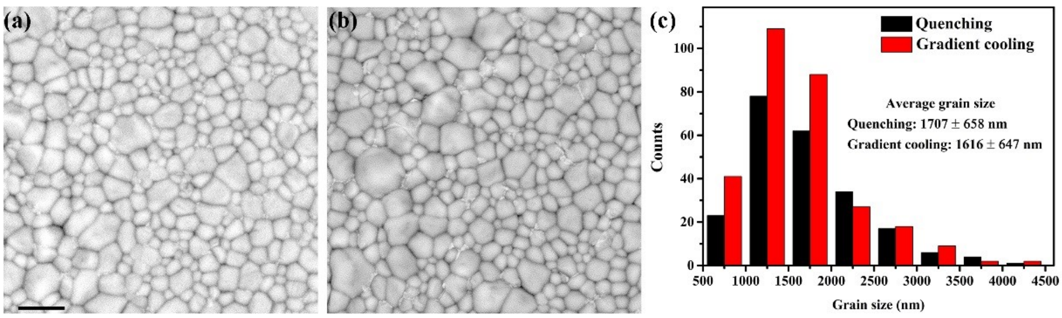

Figure S2. Top view SEM images of the quenching film (a) and gradient cooling film (b). The scale bar is 2 μm. (c) Grain size distribution histograms of perovskite films prepared by different cooling processes.

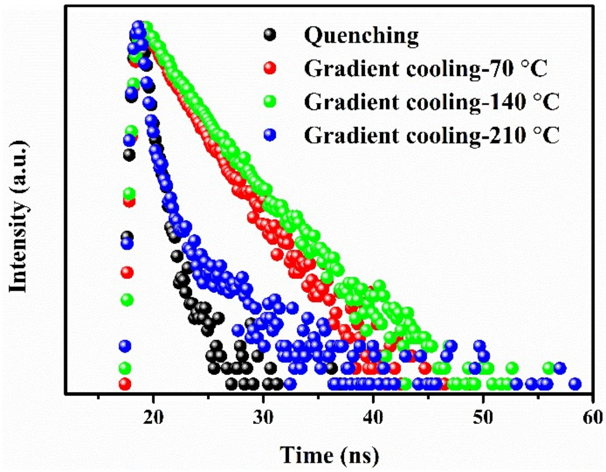

Figure S3. PL decay curves of perovskite films obtained from different cooling processes. The substrate was glass.

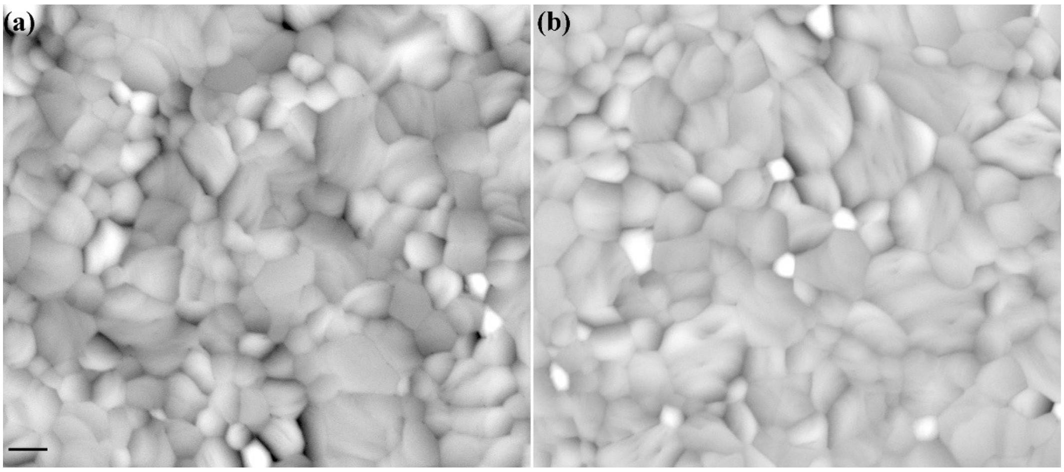

Figure S4. Top-view SEM images of perovskite films on the glass substrates. (a) The quenching film. (b) The gradient cooling film. The scale bar is 2 μm.

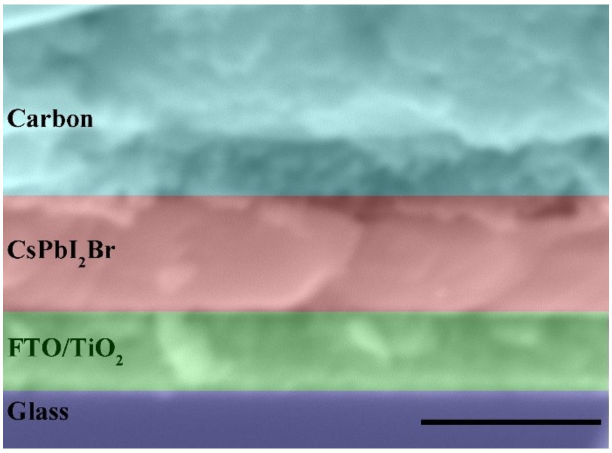

Figure S5. Cross-sectional SEM image of the device. The scale bar is 1 μm.

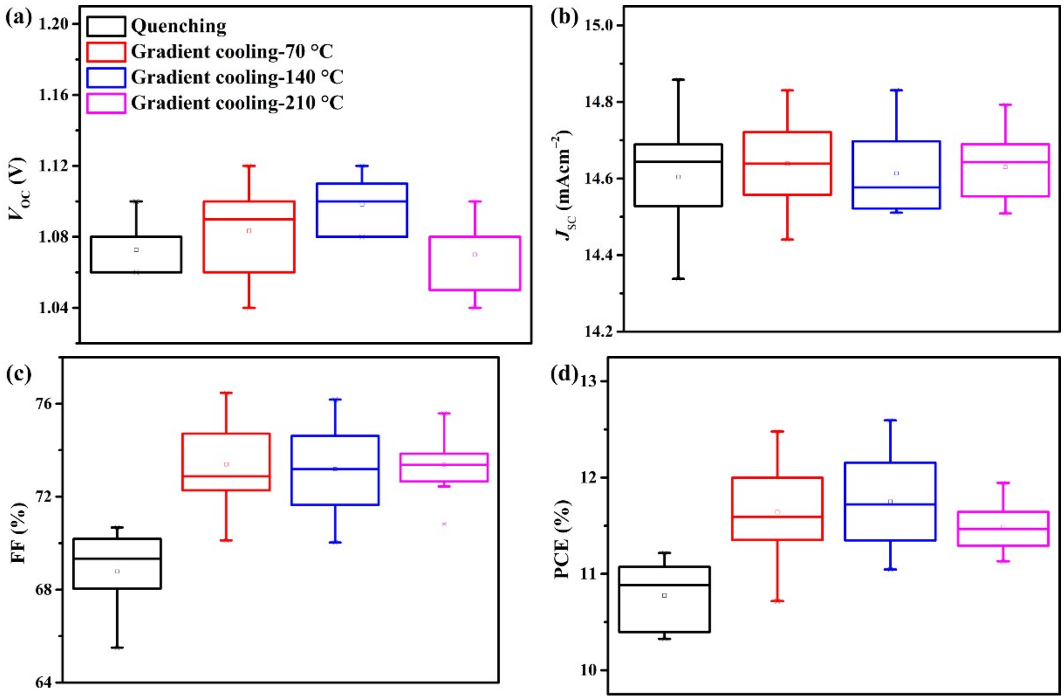

Figure S6. Box charts of photovoltaic parameters obtained from devices under different cooling conditions. (a) V_{OC}; (b) J_{SC}; (c) FF; (d) PCE.

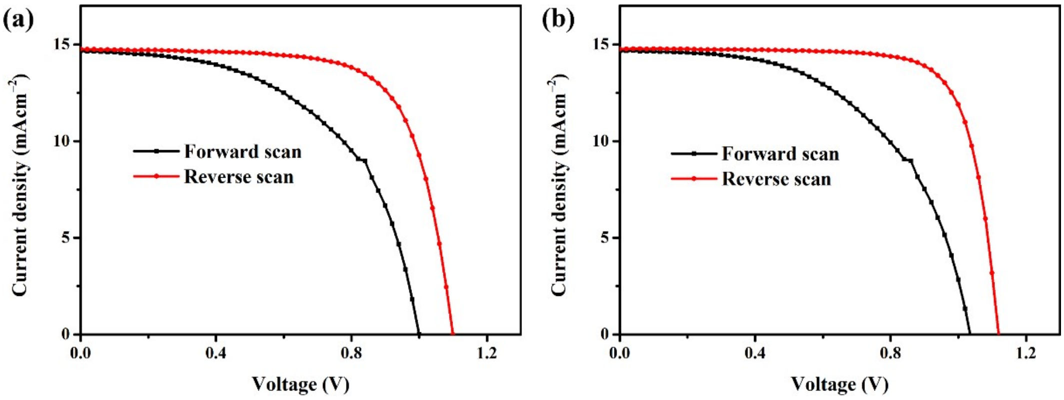

Figure S7. *J-V* curves under forward and reverse scanning for champion devices using quenching process (a) and gradient cooling process (b).

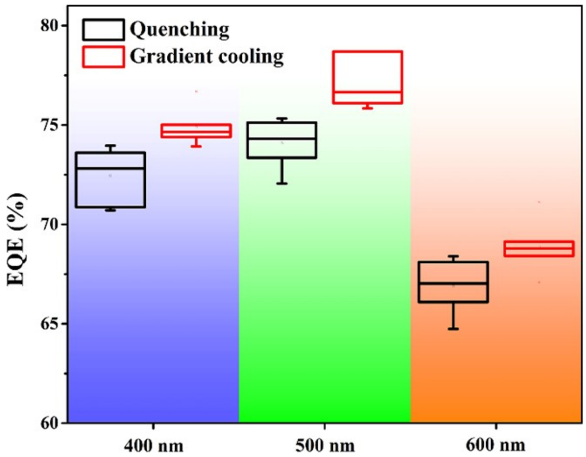

Figure S8. Statistical distribution of EQE values at three typical wavelengths (400 nm, 500 nm, and 600 nm).

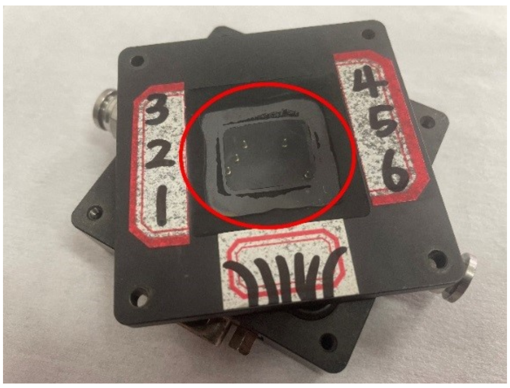

Figure S9. Optical photograph of test fixture for EQE measurement. The part in the red circle is the capping glass.

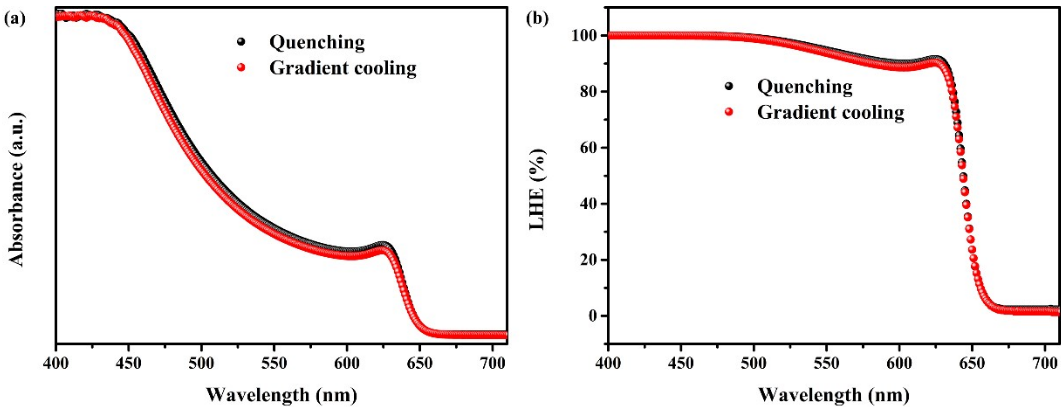

Figure S10. Absorption spectra (a) and corresponding LHE spectra (b) of perovskite films.

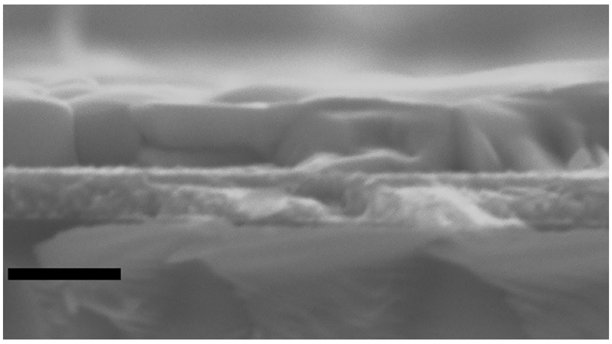

Figure S11. Cross-sectional SEM image of thick perovskite film. The scale bar is 1 μm.

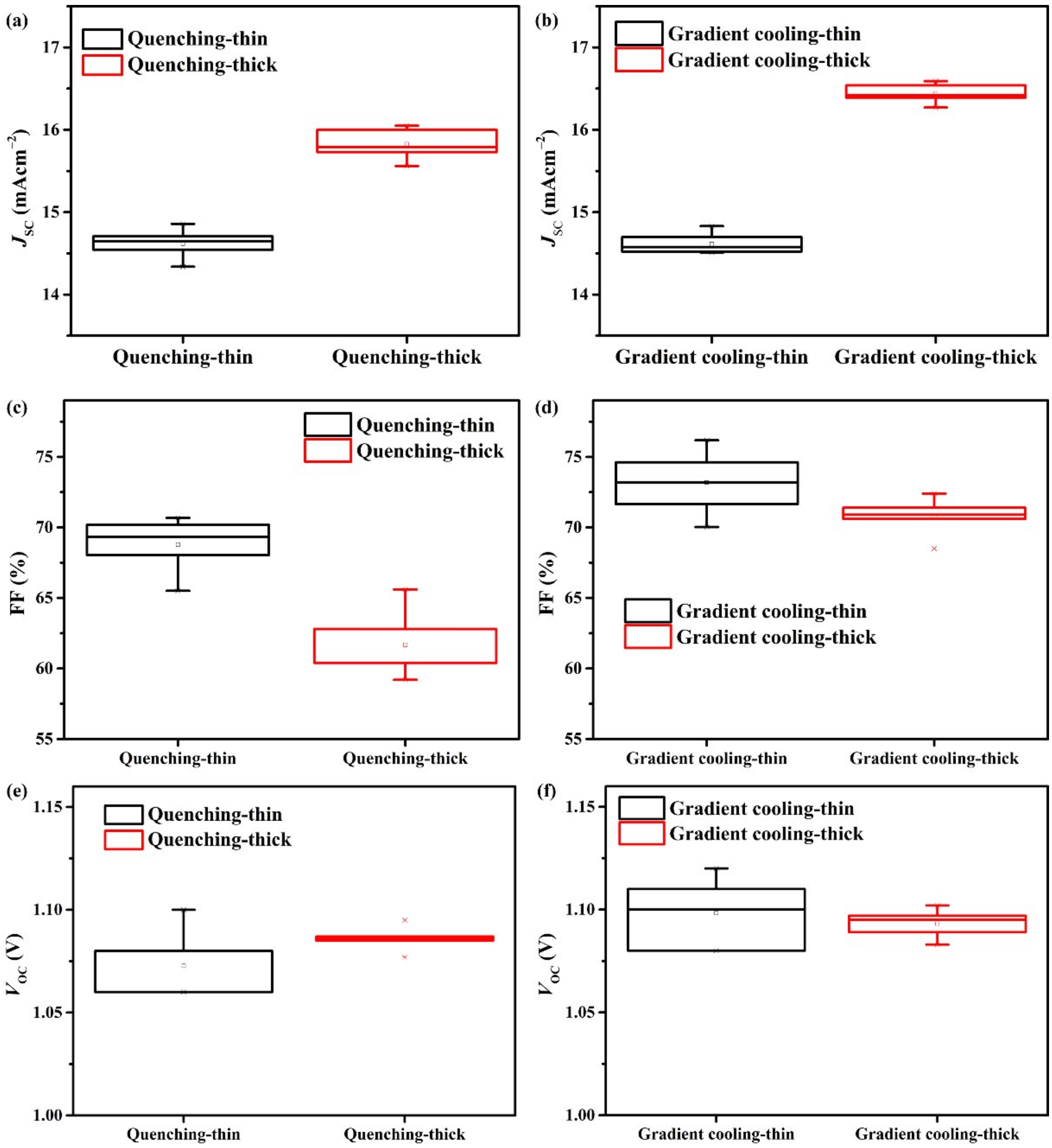

Figure S12. Comparison of photovoltaic parameters between thin and thick perovskite films. (a, b) J_{SC}; (c, d) FF; (e, f) V_{OC}.

Table S1. TRPL fitting parameters of $CsPbI_2Br$ films fabricated on different substrates.

Samples	Substrates	A_1 [%]	τ_1 [ns]	A_2 [%]	τ_2 [ns]	τ_{ave} [ns]
Quenching	glass	90.9	0.50	9.1	1.55	0.75
	FTO/TiO_2	64.4	5.93	35.6	13.61	10.23
Gradient cooling-140 °C	glass	80.7	2.80	19.3	5.78	3.78
	FTO/TiO_2	89.9	0.30	10.1	1.59	0.79
Gradient cooling-210 °C	glass	95.5	0.48	4.5	3.48	1.25
Gradient cooling-70 °C	glass	80.6	2.38	19.4	4.82	3.18

Table S2. Photovoltaic parameters of devices obtained from different cooling processes.

Devices		J_{SC} [mAcm^{-2}]	V_{OC} [V]	FF [%]	PCE [%]
Quenching	average	14.62±0.15	1.07±0.02	68.91±1.67	10.83±0.38
	best	14.77	1.10	70.30	11.42
Gradient cooling-70 °C	average	14.64±0.12	1.08±0.02	73.39±1.83	11.64±0.46
	best	14.64	1.12	76.11	12.48
Gradient cooling-140 °C	average	14.61±0.11	1.10±0.02	73.19±1.92	11.75±0.47
	best	14.76	1.12	76.18	12.59
Gradient cooling-210 °C	average	14.63±0.09	1.07±0.02	73.39±1.30	11.49±0.27
	best	14.69	1.10	73.93	11.95

Table S3. EIS fitting parameters.

Devices	R_S [Ω]	R_{CT} [Ω]	R_{rec} [Ω]	$CPE\text{-}T_1$ [F]	$CPE\text{-}T_2$ [F]
Quenching	29.89	413	1188	1.38×10^{-8}	1.12×10^{-9}
Gradient cooling	26.42	310.7	9696	3.54×10^{-8}	4.03×10^{-9}

Table S4. Photovoltaic parameters of thick devices.

Devices		J_{SC} [mAcm^{-2}]	V_{OC} [V]	FF [%]	PCE [%]
Quenching	average	15.83±0.20	1.09±0.01	61.68±2.55	10.60±0.56
	best	16.00	1.10	65.60	11.49
Gradient cooling	average	16.44±0.13	1.09±0.01	70.76±1.44	12.72±0.34
	best	16.59	1.09	72.40	13.07

Table S5. Summary of PCEs for $CsPbI_2Br$ based C-PSCs.

Device structure	**PCE [%]**	**Ref.**
FTO/c-TiO_2/$CsPbI_2Br$ (MABr top-seeded)/C	14.84	[1]
ITO/TiO_2/$CsPbI_2Br$/ATHPBr/C	14.50	[2]
FTO/c-TiO_2/m-TiO_2/$CsPbI_2Br$-CdSe QD/C	14.49	[3]
FTO/ $TiCl_4$-$TiCl_3$ modified c-TiO_2/$CsPbI_2Br$/C	14.46	[4]
FTO/TiO_2/$CsPbI_2Br$/ HTAB/C	14.30	[5]
ITO/SnO_2/$SnCl_2$/ $CsPbI_2Br$/ $BMIMBF_4$/C	14.03	[6]
ITO/SnO_2/$SnCl_2$/ $CsPbI_2Br$/ delta-2:2-bis (1,3-dithiazole) /C	13.78	[7]
ITO/SnO_2/$SnCl_2$/ $CsPbI_2Br$/ Cs_2PtI_6 /C	13.69	[8]
FTO/SnO_2/$CsPbI_2Br$-PANI/C	13.52	[9]

FTO/SnO_2/ $CsPbI_2Br$ /PEAI/C	13.38	[10]
FTO/TiO_2/ $CsPbI_2Br$ (water-based spray-assisted growth)/C	13.30	[11]
FTO/TiO_2/$CsPbI_2Br$/CuPc/C	13.16	[12]
FTO/c-TiO_2/m-TiO_2/$CsPbI_2Br$/Carbon black/C	13.13	[13]
FTO/c-TiO_2/$CsPbI_2Br$-Mg$(Ac)_2$/C	13.08	[14]
FTO/c-TiO_2/$CsPbI_2Br$ (gradient cooling)/C	13.07	This work
FTO/TiO_2/$CsPbI_2Br$-excess PbI_2/C	12.78	[15]
FTO/SnO_2/ $CsPbI_2Br$-excess PbI_2/C	12.19	[16]

References (Supporting Information)

[1] Zhu, W.; Chai, W.; Chen, D.; Ma, J.; Chen, D.; Xi, H.; Zhang, J.; Zhang, C.; Hao, Y. High-Efficiency (>14%) and Air-Stable Carbon-Based, All-Inorganic $CsPbI_2Br$ Perovskite Solar Cells through a Top-Seeded Growth Strategy. *ACS Energy Lett.* **2021,** *6* (4), 1500-1510.

[2] Yan, Z.; Wang, D.; Jing, Y.; Wang, X.; Zhang, H.; Liu, X.; Wang, S.; Wang, C.; Sun, W.; Wu, J.; Lan, Z. Surface Dipole Affords High-Performance Carbon-Based $CsPbI_2Br$ Perovskite Solar Cells. *Chem. Eng. J.* **2022,** *433*, 134611.

[3] Xu, S.; Kang, C.; Huang, Z.; Zhang, Z.; Rao, H.; Pan, Z.; Zhong, X. Dual-Functional Quantum Dot Seeding Growth of High-Quality Air-Processed $CsPbI_2Br$ Film for Carbon-Based Perovskite Solar Cells. *Sol. RRL* **2022,** 2100989.

[4] Wang, W.; Lin, Y.; Zhang, G.; Kang, C.; Pan, Z.; Zhong, X.; Rao, H. Modification of Compact TiO_2 Layer by $TiCl_4$-$TiCl_3$ Mixture Treatment and Construction of High-

Efficiency Carbon-Based $CsPbI_2Br$ Perovskite Solar Cells. *J. Energ. Chem.* **2021,** *63*, 442-451.

[5] Zhang, G.; Xie, P.; Huang, Z.; Yang, Z.; Pan, Z.; Fang, Y.; Rao, H.; Zhong, X. Modification of Energy Level Alignment for Boosting Carbon-Based $CsPbI_2Br$ Solar Cells with 14% Certified Efficiency. *Adv. Funct. Mater.* **2021,** *31* (19), 2011187.

[6] Yu, F.; Han, Q.; Wang, L.; Yang, S.; Cai, X.; Zhang, C.; Ma, T. Surface Management for Carbon-Based $CsPbI_2Br$ Perovskite Solar Cell with 14% Power Conversion Efficiency. *Sol. RRL* **2021,** *5* (9), 2100404.

[7] Han, Q.; Yang, S.; Wang, L.; Yu, F.; Zhang, C.; Wu, M.; Ma, T. The Sulfur-Rich Small Molecule Boosts the Efficiency of Carbon-Based $CsPbI_2Br$ Perovskite Solar Cells to Approaching 14%. *Sol. Energy* **2021,** *216*, 351-357.

[8] Han, Q.; Yang, S.; Wang, L.; Yu, F.; Cai, X.; Ma, T. A Double Perovskite Participation for Promoting Stability and Performance of Carbon-Based $CsPbI_2Br$ Perovskite Solar Cells. *J. Colloid Interface Sci.* **2022,** *606*, 800-807.

[9] Liu, C.; He, J.; Wu, M.; Wu, Y.; Du, P.; Fan, L.; Zhang, Q.; Wang, D.; Zhang, T. All-Inorganic $CsPbI_2Br$ Perovskite Solar Cell with Open-Circuit Voltage over 1.3 V by Balancing Electron and Hole Transport. *Sol. RRL* **2020,** *4* (7), 2000016.

[10] Zhang, Z.; Ba, Y.; Chen, D.; Ma, J.; Zhu, W.; Xi, H.; Chen, D.; Zhang, J.; Zhang, C.; Hao, Y. Generic Water-Based Spray-Assisted Growth for Scalable High-Efficiency Carbon-Electrode All-Inorganic Perovskite Solar Cells. *iScience* **2021,** *24* (11), 103365.

[11] Xie, P.; Zhang, G.; Yang, Z.; Pan, Z.; Fang, Y.; Rao, H.; Zhong, X. Perovskite-Compatible Carbon Electrode Improving the Efficiency and Stability of $CsPbI_2Br$ Solar Cells. *Sol. RRL* **2020,** *4* (11), 2000431.

[12] Gong, S.; Li, H.; Chen, Z.; Shou, C.; Huang, M.; Yang, S. $CsPbI_2Br$ Perovskite Solar Cells Based on Carbon Black-Containing Counter Electrodes. *ACS Appl. Mater. Interfaces* **2020,** *12* (31), 34882-34889.

[13] Zhang, K.; Li, W.; Yu, J.; Han, X. Magnesium Acetate Additive Enables Efficient and Stable Carbon Electrode Based $CsPbI_2Br$ Perovskite Solar Cells. *Sol. Energy* **2021,** *222*, 186-192.

[14] Wang, K.; You, T.; Yin, R.; Fan, B.; Liu, J.; Cui, S.; Chen, H.; Yin, P. Precise Nucleation Regulation and Defect Passivation for Highly Efficient and Stable Carbon-Based $CsPbI_2Br$ Perovskite Solar Cells. *ACS Appl. Energy Mater.* **2021,** *4* (4), 3508-3517.

[15] Liu, C.; Wu, M.; Wu, Y.; Wang, D.; Zhang, T. Efficient All-Inorganic $CsPbI_2Br$ Perovskite Solar Cell with Carbon Electrode by Revealing Crystallization Kinetics and Improving Crystal Quality. *J. Power Sources* **2020,** *447*, 227389.

[16] Wu, Y.; Zhang, Q.; Fan, L.; Liu, C.; Wu, M.; Wang, D.; Zhang, T. Surface Reconstruction-Induced Efficient $CsPbI_2Br$ Perovskite Solar Cell Using Phenylethylammonium Iodide. *ACS Appl. Energy Mater.* **2021,** *4* (6), 5583-5589.